Electron and neutrino scattering in the Δ-resonance region and beyond

Maria B. Barbaro[1], J.E. Amaro[2], J.A. Caballero[3], and C. Maieron[4]

[1] Università di Torino and INFN, Sezione di Torino, Italy
[2] Departamento de Física Atómica, Molecular y Nuclear, Universidad de Granada,Spain
[3] Departamento de Física Atómica, Molecular y Nuclear, Universidad de Sevilla, Spain
[4] Università di Lecce and INFN, Sezione di Lecce, Italy

Abstract. We present a unified relativistic approach to inclusive electron scattering based on the relativistic Fermi gas model and on a phenomenological extension of it which accounts for the superscaling behaviour of (e, e') data. We present results in the Δ resonance region and in the highly inelastic domain and show some application to neutrino scattering.

1 Introduction

Electron scattering off complex nuclei is an ideal testing ground for modeling neutrino-nucleus cross sections, whose accurate prediction is necessary for the analysis of on-going experimental studies of neutrino oscillations at GeV energies, presently being pursued in the MiniBooNE and K2K/T2K experiments [1, 2].

Indeed inclusive electron (e, e') and charged-current (CC) neutrino (ν_l, l^-) are closely related processes: in first Born approximation they involve the response of the nuclear system to a virtual boson, a photon or a W^+, probing the electromagnetic and weak nuclear currents, respectively.

Since the typical neutrino energies in oscillation experiments are of a few GeV, we will focus our attention on this kinematical domain. In this case the inclusive (l, l') cross section shows a pronounced peak, the so-called quasielastic peak (QEP), at an energy transfer $\omega \sim \sqrt{q^2 + m_N^2} - m_N$, corresponding to the quasi-free interaction with the individual nucleons in the nucleus (here m_N = nucleon mass). For high values of the momentum transfer $q = |\mathbf{q}|$ and higher energy loss it is possible to produce real pions and the cross section shows a second peak dominated by the resonant production of a $\Delta(1232)$ at $\omega \sim \sqrt{q^2 + m_\Delta^2} - m_N$, where m_Δ is the Δ mass. The width of these peaks is related to the Fermi momentum of the nucleons inside the nucleus and, in the case of the Δ-peak, also to the decay width of the Δ in nuclear matter. Hence for a high enough value of q, these two peaks actually overlap and cannot be separated in inclusive experiments. At higher energy transfer the so-called second resonance region is found, where the $N^*(1440)P_{11}$ (Roper), $N^*(1520)D_{13}$ and $N^*(1535)S_{11}$ resonances are excited, evolving, at very high energies, into the Deep Inelastic Scattering (DIS) regime.

Understanding the above spectrum in a unified framework has been the aim of some recent studies, which will be briefly summarized in this contribution. We shall

mainly address the electron scattering problem, where more data are available, and mention some applications to neutrino reactions.

2 The Δ resonance region

Since the kinematical domain we are exploring involves energy and momentum transfers of the order of (or higher than) the nucleon mass, the traditional non-relativistic approach is bound to fail and a relativistic approach to the problem is required.

A fully relativistic treatment of the nuclear many-body system is a longstanding and extremely difficult task that is best pursued in special frameworks like the Relativistic Fermi Gas (RFG) model, where basic symmetries like Lorentz covariance and gauge invariance are exactly respected.

Hence we assume as a starting point an extension of the RFG model, which has been widely employed in the QEP, to the inelastic region. In this model, the virtual boson is absorbed by an on-shell nucleon described by a Dirac spinor $u(\mathbf{h}, s_h)$, with energy $\overline{E}_{\mathbf{h}} = \sqrt{\mathbf{h}^2 + m_N^2}$.

The basic ingredient of the calculation is the hadronic tensor $\mathcal{W}^{\mu\nu}$, which contains all the information on the nuclear structure and dynamics and yields the (e, e') differential cross section with respect to the lepton final energy ε_f and solid angle Ω_f according to the follwing relation

$$\frac{d\sigma}{d\Omega_f d\varepsilon_f} = \frac{2\alpha^2}{Q^4}\frac{\varepsilon_f}{\varepsilon_i}\eta_{\mu\nu}\mathcal{W}^{\mu\nu} \ , \tag{1}$$

where α is the fine structure constant, ε_i the lepton initial energy, $\eta_{\mu\nu}$ the leptonic tensor and $Q_\mu = (\omega, \mathbf{q})$ the four-momentum transfer.

For the excitation of a stable resonance N^* of mass m^* the RFG hadronic tensor turns out to be [3]

$$\mathcal{W}^{\mu\nu}_{*,RFG}(q, \omega, m^*) = \frac{3\mathcal{N}}{4\kappa m_N \eta_F^3}\xi_F\, \Theta(1 - \psi^{*2})(1 - \psi^{*2})U^{\mu\nu}_*(q, \omega, m^*) \tag{2}$$

where $\mathcal{N}$ is the number of nucleons involved in the reaction, $\kappa = q/2m_N$ and $\eta_F = \sqrt{\xi_F(\xi_F + 2)} = k_F/m_N$ are the dimensionless transferred and Fermi momentum, respectively, and the "single-nucleon" tensor $U^{\mu\nu}_*$ embeds the information about the $N - N^*$ transition *.

In analogy with the physics of the quasi-elastic peak [5], a *scaling variable* ψ^*, defined as follows

$$\psi^* \equiv \psi(\kappa, \lambda; m^*) = \pm\sqrt{\frac{1}{\xi_F}\left[\kappa\sqrt{\frac{1}{\tau} + \rho(m^*)^2} - \lambda\rho(m^*) - 1\right]} \ , \tag{3}$$

* Actually in a fully relativistic framework the single nucleon physics cannot be exactly disentagled from the many-body part of the problem and the tensor $U^{\mu\nu}_*$ contains corrections due to the medium (see, e.g., ref. [4]).

with $\lambda = \omega/2m_N$ and $\tau = \kappa^2 - \lambda^2$, has been introduced. The quantity

$$\rho(m^*) = 1 + \frac{1}{4\tau}\left(m^{*2}/m_N^2 - 1\right) \ , \tag{4}$$

measures the inelasticity of the elementary process and reduces to 1 in the quasielastic limit $m^* = m_N$. The physical meaning of the scaling variable ψ^* is the following: $\xi_F \psi^{*2}$ represents the minimum kinetic energy required to transform a nucleon inside the nucleus into a resonance N^* when hit by a photon of energy λ and momentum κ. In terms of the scaling variable the RFG response region associated to a specific resonance is $-1 \leq \psi^* \leq 1$ and the peak position corresponds to $\psi^* = 0$.

A realistic model for the resonance requires the inclusion of the decay width Γ in the hadronic tensor. This can be computed from the tensor $\mathcal{W}_*^{\mu\nu}(q,\omega,W)$ for a stable N^* with mass W by a convolution

$$\mathcal{W}_\Gamma^{\mu\nu}(q,\omega) = \int_{W_{min}}^{W_{max}} \frac{1}{\pi} \frac{\Gamma(W)/2}{(W-m^*)^2 + \Gamma(W)^2/4} \mathcal{W}_*^{\mu\nu}(q,\omega,W) dW \ , \tag{5}$$

where the integration interval goes from threshold to the maximum value allowed in the Fermi gas model.

The above expressions are independent of the specific transition under consideration: they can be used to describe the Δ, the $N^*(1440)$ or any other resonance region [6,7] (after modifying m^* and $\Gamma(W)$ accordingly) as well as the quasielastic peak (in the $\Gamma \to 0$ limit setting $m^* = m_N$) [8].

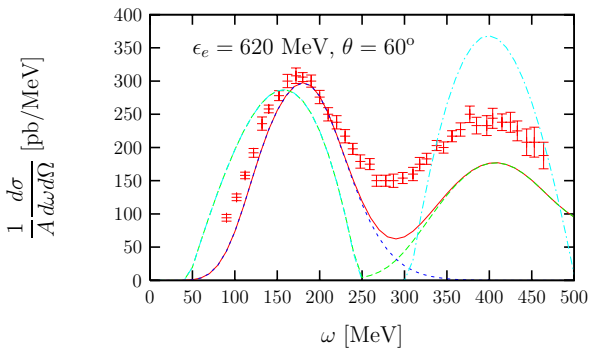

Figure 1. Inclusive cross section per nucleon from ^{12}C. Llight blue: RFG without Δ width; green: RFG including the finite Δ width; blue: PWIA for the quasi-elastic peak; red: hybrid model obtained by adding the PWIA cross section in the quasi-elastic peak and RFG cross section in the Δ-peak. Experimental data are taken from [9].

As already mentioned the specific transition form factors are hidden in the tensor $U_*^{\mu\nu}$. Concerning the Δ resonance, a relativistic calculation of the (e,e') response in this region must use the full $N \to \Delta$ vertex, which includes the magnetic (M1),

electric (E2) and Coulomb (C2) excitation amplitudes. Although for years an important program has been pursued to determine more accurately the quadrupole $C2$ and $E2$ amplitudes in the Δ region (these being small compared with the dominant dipole $M1$ amplitude), our knowledge is still incomplete and has not been possible to undertake a full analysis in the sense of the work by Nozawa and Lee [10] of the effect of the C2 and E2 form factors in the nuclear Δ-peak. Accordingly we use the parameterization [11] $G_{E,M}(Q^2) = G_{E,M}(0)G_E^P(Q^2)/\sqrt{1-Q^2/(3.5GeV/c)^2}$, namely we assume that the same dependence in Q^2 is valid for the electric and magnetic form factors and that the isobar form factor falls off faster than the proton form factor.

In Fig. 1 we show results for the nuclear inclusive cross section per nucleon from ^{12}C compared with the experimental data. Light-blue lines correspond to the RFG for a stable Δ. The width is included in the green line result according to eq. (5) and produces a broadening of the Δ peak and correspondingly a decrease of the strength. As an illustration of how one could improve the model in the quasi-elastic-peak region, we also show with blue lines the quasi-elastic cross section computed with the semirelativistic PWIA model of ref. [12], which includes the momentum distribution of the finite-sized nucleus, producing the "tails" of the cross section, and the binding energy of the nucleons in the nucleus, yielding a shift to higher energies. Finally, we show with red lines the results computed with a hybrid model in which we add the PWIA cross section for the quasi-elastic contribution to the RFG result for the Δ contribution.

As we can see in Fig. 1, our results are below the data in the dip and Δ region. This was expected because other contributions coming mainly from two-nucleon emission and non-resonant pion production (not included in our model) also enter here.

In Ref. [6] several relativistic effects and ingredients of the calculation were analyzed in detail. Here we just like to stress two basic findings. First, from a comparison between different Lagrangians in the treatment of the Δ excitation, it emerges that the Peccei Lagrangian [13], employed in the pioneering calculation by Moniz [14], is only appropriate for computing the transverse response for low momentum transfer, but in the longitudinal channel the full vertex [15]

$$\langle \Delta | j_\mu | N \rangle = \overline{u}^\beta_\Delta \left(C_1 \Gamma^1_{\mu\beta} + C_2 \Gamma^2_{\mu\beta} + C_3 \Gamma^3_{\mu\beta} \right) u \ , \tag{6}$$

(where u^β_Δ is the Rarita-Schwinger spinor describing a spin 3/2 particle) should be retained: indeed the Peccei Lagrangian, corresponding to the first term Γ^1 only, gives an unreasonably large longitudinal response. Second, we have found a large sensitivity of the longitudinal response to the inclusion of the Coulomb form factor of the isobar, especially for high q, a fact that could be of importance for investigations of the longitudinal nuclear response. On the other hand, both longitudinal and transverse responses are found to be insensitive to the quadrupole E2 form factor.

Let us now briefly comment on the second resonance region, namely where resonances heavier than the Δ are found. Among these, the $N^*(1440)P_{11}$ (the so-called Roper resonance), occurring just above the Δ(1232), is particularly interest-

ing, since it can be viewed as a radial excitation of a three-quark nucleon state, analog of the breathing mode of the nucleus, hence carrying information on the nucleon's compressibility. A first step towards a theoretical description of the nuclear response functions in the Roper resonance region was made in ref. [7], where the corresponding RFG responses were calculated within several different theoretical models for the electroproduction amplitudes. In particular it was shown that, although the experimental information was still insufficient to allow a stringent test of the various theories, the longitudinal response R_L associated with the Roper can be large compared with the contribution arising from the Δ near the light-cone and that that the impact of the Roper on the Coulomb sum rule can be significant.

3 The highly inelastic region

To study what we call the "highly inelastic" domain, namely the region beyond the resonances, we assume that the final state can be described in terms of a recoiling nuclear state plus a highly inelastic state of mass m^*. In this case the RFG hadronic tensor can be written as [3]

$$\mathcal{W}^{\mu\nu}_{inel,RFG}(q,\omega) = \frac{3\mathcal{N}\tau\xi_F}{2\kappa m_N \eta_F^3}\int_{\rho_1}^{\rho_2} d\rho\Theta(1-\psi^{*2})(1-\psi^{*2})U^{\mu\nu}_{inel}(q,\omega,m^*) \quad (7)$$

where ρ_1 and ρ_2 are the kinematical boundaries at fixed q and ω. Thus for each value of ρ (and hence m^*) a "peak" can be identified, corresponding to the region $-1 \leq \psi^* \leq 1$, centered at $\psi^* = 0$, whose width is a function that grows with q and decreases with m^*. The single-nucleon inelastic hadronic tensor $U^{\mu\nu}_{inel}$ can be parameterized in terms of two structure functions, w_1 and w_2 (see ref. [3]). In computing it we employ phenomenological fits of the single-nucleon inelastic structure functions measured in DIS experiments. Among the various parameterizations which can be found in the literature here we adopt the Bodek *et al.* fit of [17], which describes both the deep inelastic and resonance regions.

Once the inelastic RFG modeling is in hand, we can go beyond this simple non-interacting model, still retaining its relativistic content. This we do by exploiting the so-called "superscaling" behavior of inclusive lepton-nucleus reactions. We shall see that this has a significant impact on the nuclear responses at high inelasticity.

In order to introduce the concept of superscaling, we observe that Eq. (2) can be recast in the form

$$\mathcal{W}^{\mu\nu}_{*,RFG}(q,\omega,m^*) = f_{RFG}(\psi^*) \times G^{\mu\nu}(q,\omega,m^*)\,, \quad (8)$$

where

$$f_{RFG}(\psi^*) = \frac{3}{4}\Theta(1-\psi^{*2})(1-\psi^{*2}) \quad (9)$$

is the RFG *superscaling function*: hence by dividing the RFG nuclear tensor by an appropriate tensor $G^{\mu\nu}$ - whose definition follows immediately from Eqs. (2) and (8) - a universal function f_{RFG} is obtained, which does not depend on the

three variables q, ω and k_F independently, but only upon one specific combination, namely the scaling variable (3).

As a consequence the RFG model predicts that if the inclusive cross section is divided by an appropriate function and plotted versus the corresponding scaling variable, no dependence on the momentum transfer q (scaling of the first kind) nor on the target nucleus, specified by the fermi momentum k_F (scaling of the second kind), is found. The simultaneous occurrence of the two kinds of scaling is known as *superscaling*.

In the quasielastic peak domain $(m^* = m_N)$, superscaling has been widely tested against the (e, e') data in Ref. [18], where it was shown that both kinds of scaling are fulfilled with a good degree of accuracy in the region $\psi < 0$ providing the momentum transfer is not too low. The scaling analysis of the separated longitudinal and transverse responses has also proved that the scaling violations observed in the $\psi > 0$ region mainly reside in the transverse channel, whereas the longitudinal data do scale rather well in the whole QE region.

However the shape of the experimental QE longitudinal superscaling function differs from the RFG parabolic one, extending outside the region $-1 < \psi < 1$ and, most importantly, displaying an asymmetry around the QEP with a pronounced tail in the $\psi > 0$ region. The asymmetry of the superscaling function has been and still is the object of many investigations [19–23] and represents a stringent constraint that any realistic nuclear model aiming to describe (l, l') reactions should fulfill.

An expression for a phenomenological QE longitudinal scaling function, $f_{QE}(\psi)$, was obtained by fitting the data [24]. Based on these results, we now make the following hypothesis: we assume that $f_{QE}(\psi)$ provides a good description of $f(\psi^*) = f_L(\psi^*) = f_T(\psi^*)$ ("scaling of the zeroth kind"), as it implicitly contains the initial-state physics, and thus we make, *for any* m^*, the following substitution:

$$f_{RFG}(\psi^*) \to f_{QE}(\psi^*) \ . \tag{10}$$

The corresponding results are illustrated in Fig. 2, where the inclusive cross section is shown together with the separated QE and inelastic contributions for a ^{12}C target at $E_{inc} = 4.045$ GeV and $\theta_e = 15°$ (a), $30°$ (b), $45°$ (c) and $74°$ (d), The calculation was performed in the Relativistic Fermi Gas including a phenomenological energy shift (red lines) and in the phenomenological extension of it (magenta lines), which we denote here as ERFG (Extended Relativistic Fermi Gas), based on the fit of the quasielastic scaling function f_{QE} [24].

We notice that for low scattering angle (a) the RFG model yields roughly the right position and height of the QE peak, but fails to reproduce the tails of the peak, giving in particular an unobserved dip at $\omega \simeq 800$ MeV. On the other hand the ERFG, while reproducing the data in the tails better, significantly underestimates the cross section at the peak. This is related to the fact that the peak of the phenomenological function f_{QE} is lower than the corresponding RFG value. For higher angles [Figs. 2 (b),(c),(d)] the data lie roughly in between the predictions of ERFG (smaller) and RFG (larger) models, the former again reproducing the low-ω behavior better. As a general result we observe that as the scattering angle increases the range of validity of the ERFG also increases.

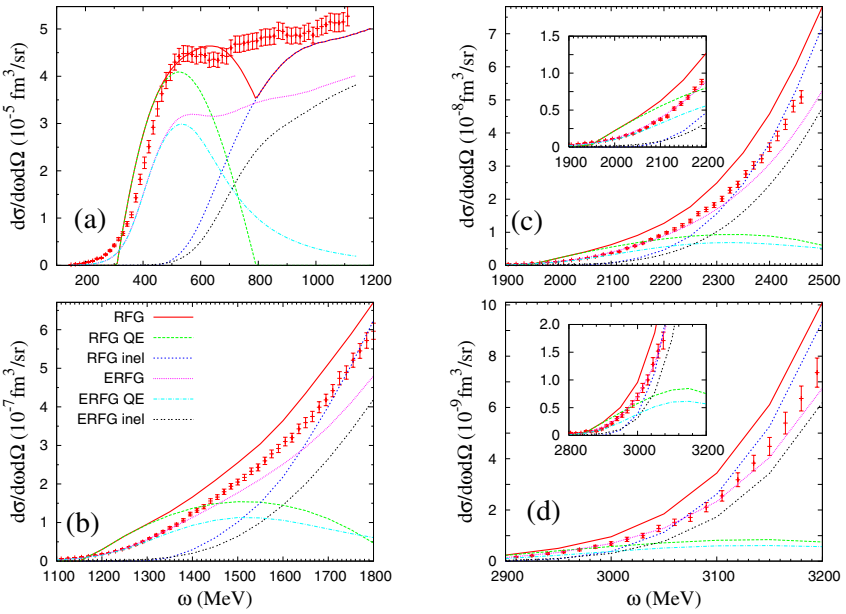

Figure 2. Inclusive cross section for electron scattering from carbon at $E_{inc} = 4.045$ GeV and $\theta_e = 15°$ (a), $30°$ (b), $45°$ (c) and $74°$ (d), versus the energy transfer. Red: RFG; magenta: ERFG. The calculation includes an energy shift $\omega_{shift} = 20$ MeV and the separate QE and inelastic contributions to the cross section are shown (dashed). Data are from [16].

An important comment is in order. The RFG and ERFG models consider here the 1p-1h one-body contributions both for elastic scattering from a nucleon in the nucleus and for representations of the single-nucleon inelastic spectrum, thereby incorporating effects from meson production, excitation of baryon resonances (notably the Δ) and, at high excitation energies, DIS. However, in this region and beyond effects arising from reaction mechanisms not included here, namely, those coming from correlations and both 1p-1h and 2p-2h meson-exchange currents can be also important [25–27] and, from some preliminary study, they tend to bring the total (the present ERFG contributions plus these additional MEC contributions) into better agreement with the data. Therefore the fact that the ERFG yields a cross section that is below the data is somehow encouraging, since this leaves room for the above-mentioned effects to provide the balance.

Similar results are obtained for the superscaling function: in Fig. 3 the total scaling function f is shown as a function of the QE variable ψ' (the "prime" indicating the inclusion of a phenomenological energy shift, needed to reproduce the QEP position) for four different nuclei, within the RFG (left panel) and ERFG (right panel) models, at $E_e = 3.595$ GeV and $\theta_e = 16^0$; experimental data are obtained from

the measured inclusive cross sections divided by the single nucleon cross section and the curves are obtained by dividing the theoretical inclusive cross section by the same quantity. A closer inspection of the transverse superscaling function $f_T(\psi')$, performed in ref. [3] at the same kinematics, shows that the discrepancy between "data" and "theory" is larger for the transverse case than for the total scaling functions at this scattering angle ($\theta = 16^0$). This indicates that extra contributions should be added to the nuclear model, going beyond the present one-body description, and that these must act mainly in the transverse channel.

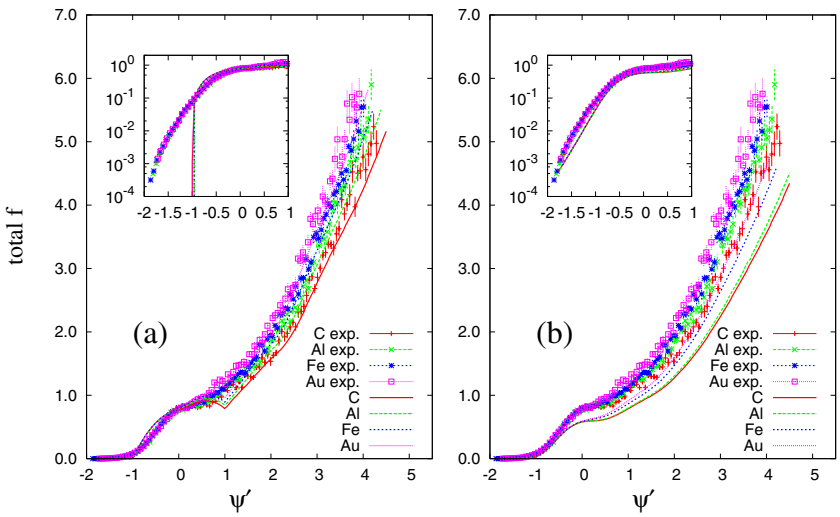

Figure 3. Total superscaling functions $f(\psi')$ for $E_e = 3.595$ GeV and $\theta_e = 16°$. Theoretical results obtained within the RFG are shown in panel (a), while the ERFG case is presented in panel (b).

4 Scaling in the Δ region and application to neutrino scattering

In the previous Section the superscaling function f_{QE} extracted from the quasielastic peak data has been used to calculate the full inelastic (e, e') spectrum. Two basic assumptions underly this approach: first that the longitudinal and transverse superscaling functions coincide (0-th kind scaling) and second that the superscaling function, embodying the nuclear initial and final state interactions, is the same in all kinematical domains, the latter being characterized only by the structure functions w_1 and w_2.

In Ref. [28] a different approach to the Δ resonance region was taken. First the contribution of the Δ has been isolated by subtracting from the total experimental cross section the quasielastic contribution, reconstructed using the superscaling

function f_{QE} introduced above. Next the left-over cross section has been divided by the appropriate $N \to \Delta$ single-nucleon cross section and the result has been displayed versus the scaling variable ψ_Δ, given by Eq. (3) when $m^* = m_\Delta$. The results are found to scale quite well [28] for $\psi_\Delta < 0$, suggesting that this procedure has indeed identified the dominant contributions not only in the QE region, but also in the Δ region. Of course for $\psi_\Delta > 0$ higher resonances come into play and this procedure is no longer correct. The residual scaling function f^Δ, whose fit is plotted in Fig. 4, while similar to f_{QE}, differs in detail: it is somewhat lower, is shifted slightly and is more spread out over a wider range of scaling variable. This is not unexpected, since implicit in this approach is the fact that the Δ brings with it its own width and shift. A microscopic analysis of f_Δ is presently being carried out [29] in order to deconvolute the width from the total response and see whether or not the underlying scaling function is indeed the basic f_{QE} deduced above.

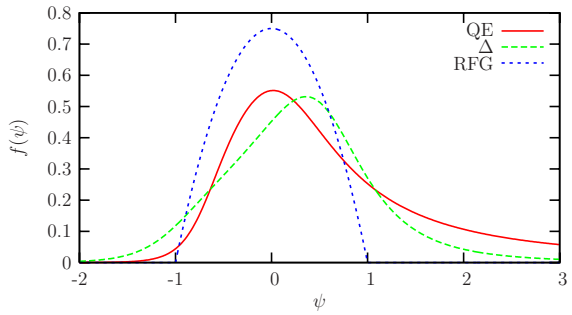

Figure 4. Fits of the superscaling function for the quasi-elastic (QE) and Δ-resonance regions plotted versus the corresponding scaling variable ψ and compared to the RFG result.

As mentioned in the introduction, a major advantage of the approach above illustrated is that the scaling functions f_{QE} and f_Δ extracted by (e, e') data can be used to predict neutrino-nucleus cross sections in both the quasielastic and Δ regions. Indeed, as tested in ref. [28] in a wide range of kinematical conditions, these phenomenological functions give *by construction* a good description of the electron scattering data and are in this sense model-independent. The so-called SuSA (SUperScaling Approximation) approach amounts to multiply the two superscaling functions for the corresponding neutrino-nucleon elementary cross section.

Several applications of the SuSA approximation to neutrino and antineutrino scattering are shown in Ref. [28]. In Fig. 5 we display, as an example, a comparison of the SuSA and RFG results, clearly showing that the relativistic Fermi gas badly overestimate the cross section in both the QE and Δ regions as compared to the phenomenological model based on superscaling.

It is worth mentioning that more fundamental approaches, based on relativistic mean field theory with final state interactions [20, 22] and on the coherent density fluctuation model (CDFM) [30, 31] and aiming to justify the properties of the exper-

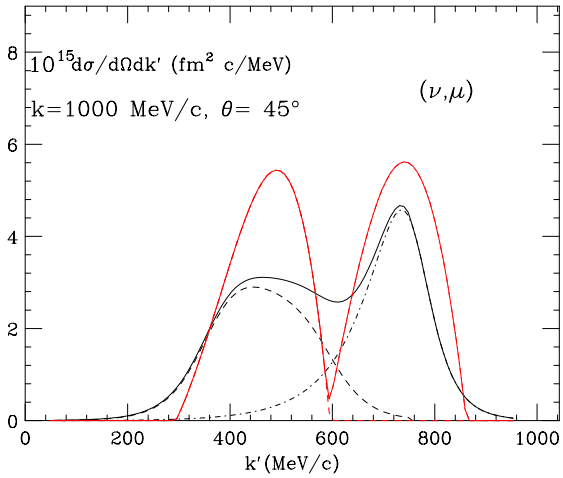

Figure 5. Neutrino reaction cross section for $E_\nu = 1$ GeV and $\theta = 45$ degrees. Red line: RFG result; black lines: SuSA result (dashed: Δ; dotdashed:quasielastic, solid:total) .

imental superscaling function, have been recently carried out both in the quasielastic and in the Δ regions and applied to neutrino reactions, leading to results similar to the ones shown in Fig. 5.

5 Conclusions

We have shown how the full inelastic spectrum of inclusive electron-nucleus scattering can be described within in a fully relativistic unified formalism which can be applied in the few GeV energy domain. The model, based on the Relativistic Fermi Gas, takes into account initial and final state interactions in a phenomenological way through the use of a superscaling function directly extracted from (e, e') data. This allows one to make model independent predictions for neutrino-nucleus cross sections, needed in the analysis of ν oscillation experiments.

References

1. A. A. Aguilar-Arevalo *et al.* [The MiniBooNE Collaboration], Phys. Rev. Lett. **98** (2007) 231801.
2. M. H. Ahn *et al.* [K2K Collaboration], Phys. Rev. D **74** (2006) 072003.
3. M. B. Barbaro, J. A. Caballero, T. W. Donnelly and C. Maieron, Phys. Rev. C **69**, 035502 (2004).
4. L. Alvarez-Ruso, M. B. Barbaro, T. W. Donnelly and A. Molinari, Phys. Lett. B **497**, 214 (2001).

5. W. M. Alberico, A. Molinari, T. W. Donnelly, E. L. Kronenberg and J. W. Van Orden, Phys. Rev. C **38**, 1801 (1988).
6. J. E. Amaro, M. B. Barbaro, J. A. Caballero, T. W. Donnelly and A. Molinari, Nucl. Phys. A **657** (1999) 161.
7. L. Alvarez-Ruso, M. B. Barbaro, T. W. Donnelly and A. Molinari, Nucl. Phys. A **724** (2003) 157.
8. T. W. Donnelly, M. J. Musolf, W. M. Alberico, M. B. Barbaro, A. De Pace and A. Molinari, Nucl. Phys. A **541** (1992) 525.
9. P. Barreau et al., Nucl. Phys. A **402** (1983) 515.
10. S. Nozawa and T.-S.H. Lee, Nucl. Phys. A **513** (1990) 511.
11. K. Wehrberger, C. Bedau and F. Beck, Nucl. Phys. A **504** (1989) 797.
12. J.E. Amaro, J.A. Caballero, T.W. Donnelly, E. Moya de Guerra, Nucl. Phys A **611** (1996) 163.
13. R.D. Peccei, Phys. Rev. **181** (1969) 1902.
14. E.J. Moniz, Phys. Rev. C **184** (1969) 1154.
15. H.F. Jones and M.D. Scadron, Ann. Phys. **81** (1973) 1.
16. J. Arrington *et al.*, Phys. Rev. Lett. **82**, 2056 (1999).
17. A. Bodek and J. L. Ritchie, Phys. Rev. D **23**, 1070 (1981); Phys. Rev. D **24**, 1400 (1981); Phys. Rev. D **20**, 1471 (1979).
18. T. W. Donnelly and I. Sick, Phys. Rev. Lett. **82**, 3212 (1999).
19. J. A. Caballero, J. E. Amaro, M. B. Barbaro, T. W. Donnelly and J. M. Udias, Phys. Lett. B **653** (2007) 366.
20. J. E. Amaro, M. B. Barbaro, J. A. Caballero, T. W. Donnelly and J. M. Udias, Phys. Rev. C **75** (2007) 034613.
21. J. E. Amaro, M. B. Barbaro, J. A. Caballero and T. W. Donnelly, Phys. Rev. Lett. **98** (2007) 242501.
22. J. A. Caballero, J. E. Amaro, M. B. Barbaro, T. W. Donnelly, C. Maieron and J. M. Udias, Phys. Rev. Lett. **95** (2005) 252502.
23. J. E. Amaro, M. B. Barbaro, J. A. Caballero, T. W. Donnelly and C. Maieron, Phys. Rev. C **71** (2005) 065501.
24. J. Jourdan, Nucl. Phys. A **603**, 117 (1996).
25. J. E. Amaro, M. B. Barbaro, J. A. Caballero, T. W. Donnelly and A. Molinari, Nucl. Phys. A **723** (2003) 181.
26. J. E. Amaro, M. B. Barbaro, J. A. Caballero, T. W. Donnelly and A. Molinari, Phys. Rept. **368** (2002) 317.
27. A. De Pace, M. Nardi, W. M. Alberico, T. W. Donnelly and A. Molinari, Nucl. Phys. A **726** (2003) 303; Nucl. Phys. A **741** (2004) 249.
28. J. E. Amaro, M. B. Barbaro, J. A. Caballero, T. W. Donnelly, A. Molinari and I. Sick, Phys. Rev. C **71** (2005) 015501.
29. C. Maieron, J. E. Amaro, M. B. Barbaro, J. A. Caballero, T. W. Donnelly, in preparation.
30. A. N. Antonov, M. V. Ivanov, M. B. Barbaro, J. A. Caballero, E. Moya de Guerra and M. K. Gaidarov, Phys. Rev. C **75** (2007) 064617.
31. A. N. Antonov *et al.*, Phys. Rev. C **74** (2006) 054603.